

## Supporting information

### Two-photon polymerisation of sugar responsive 4D microstructures

Alexa Ennis<sup>1†</sup>, Deanna Nicdao<sup>1†</sup>, Srikanth Kolagatla<sup>1</sup>, Luke Dowling<sup>2</sup>, Yekaterina Tskhe<sup>1</sup>, Alex J. Thompson<sup>3,4</sup>, Daniel Trimble<sup>2</sup>, Colm Delaney<sup>1</sup>, Larisa Florea<sup>1\*</sup>

<sup>1</sup>School of Chemistry & AMBER, The SFI Research Centre for Advanced Materials  
and BioEngineering Research, Trinity College Dublin, Dublin 2, Ireland.

E-mail: FLOREAL@tcd.ie

<sup>2</sup>Department of Mechanical & Manufacturing Engineering, Trinity College Dublin, Dublin 2, Ireland

<sup>3</sup>Department of Surgery & Cancer, Queen Elizabeth the Queen Mother Wing, St Mary's Hospital, Imperial  
College London, South Wharf Road, London, W2 1NY, United Kingdom

<sup>4</sup>The Hamlyn Centre, Institute of Global Health Innovation (IGHI), Imperial College London, Exhibition Road,  
South Kensington, London, SW7 2AZ, United Kingdom

†Both authors contributed equally to this manuscript

**Table S1.** Photoresist composition with varied IL content ( $[P_{4,4,4,4}][Cl]$ ) and laser power employed for micro-fabrication.

Composition (mol % to acrylamide)	Laser Power				
	20 mW	25 mW	30 mW	35 mW	40 mW
Photoresist 1 (40 mol % IL)	✓	✓	✓	✓	✓
Photoresist 2 (50 mol % IL)	✓	✓	✓	✓	✓
Photoresist 3 (60 mol % IL)	✓	✓	✓	✓	✓
Photoresist 4 (75 mol % IL)	✓	✓	✓	✓	✓
Photoresist 5 (85 mol % IL)	X	X	✓	✓	✓
Photoresist 6 (100 mol % IL)	X	X	X	X	✓
Photoresist 7 (150 mol % IL)	X	X	X	X	X

✓ - denotes successful fabrication of cylindrical pillars arrays (30  $\mu\text{m}$  in height, 20  $\mu\text{m}$  in diameter) as detailed in the Experimental section; all structures were developed in PGMEA/IPA and imaged to ensure structural integrity. In all cases the fabrication was performed on a Photonic Professional Nanoscribe GmbH system in oil immersion, using a 63X objective, at a scan speed of 1  $\text{mm s}^{-1}$ .

X – denotes unsuccessful fabrication

**Table S2.** Photoresist composition with varied IL content ( $[P_{4,4,4,4}][Cl]$ ) and successful micro-fabrication parameters obtained in this work.

Photoresist Name	Photoresist 1	Photoresist 2	Photoresist 3	Photoresist 4	Photoresist 5	Photoresist 6	Photoresist 7
Acrylamide (mg)	300	300	300	300	300	300	300
IL (mg)	500	623	747	934	1058	1245	1870
IL mol % in relation to acrylamide	40 mol%	50 mol %	60 mol %	75 mol %	85 mol %	100 mol %	150 mol %
IL wt% in photoresist	49.6 %	55.0 %	59.4 %	64.7 %	67.5 %	71.0 %	78.6 %
Power range* (mW)	20 – 40 mW	20 – 40 mW	20 – 40 mW	20 – 40 mW	30 – 40 mW	40 mW	N/A

\*Indicates power range for successful micro-fabrication using the experimental conditions described in this work.

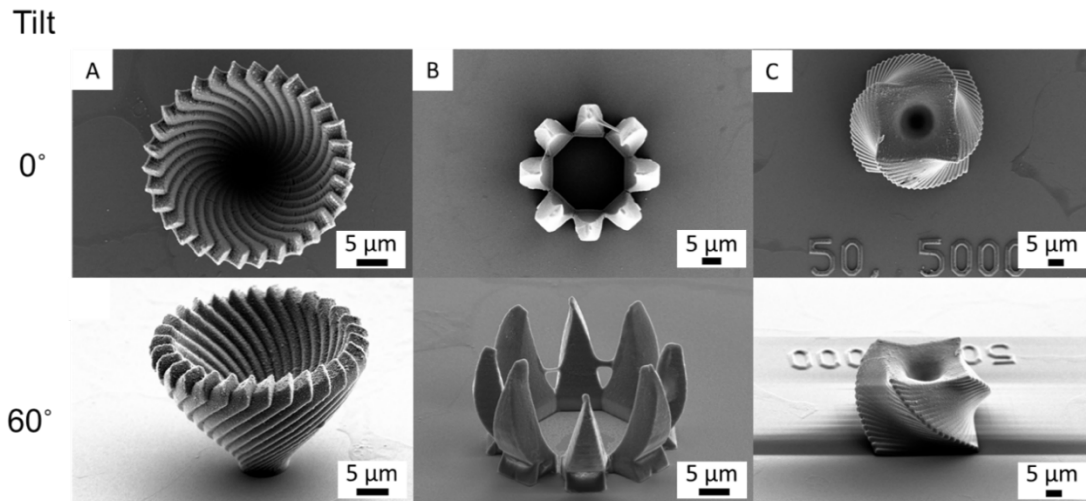


**Figure S1.** Scanning Electron Microscopy images taken from above (top-down) and at 60 ° tilt for a selection of 3D structures. A) Twisted vase structure B) Flower structure C) Rotating vase structure. All structures were fabricated using the Photonic Professional GT system (Nanoscribe GmbH) in the oil immersion configuration using a 63X oil objective and the photoresist described in Table 1.

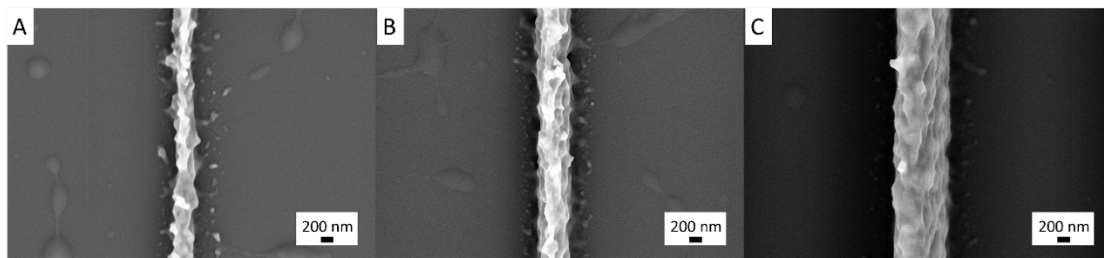


**Figure S2.** Scanning Electron Microscopy images of single line fabricated at A) laser power of 15 mW and scan speed 20 mm s<sup>-1</sup>; B) laser power 15 mW and scan speed 10 mm s<sup>-1</sup>; C) laser power 20 mW and scan speed 5 mm s<sup>-1</sup>. Line widths approximately A) 893.99 nm (± 13.85 nm); B) 518.45 nm (± 42.25 nm); C) 293.97 nm (± 59.19 nm). Line widths were calculated using 5 measurements for each set of fabrication parameters.

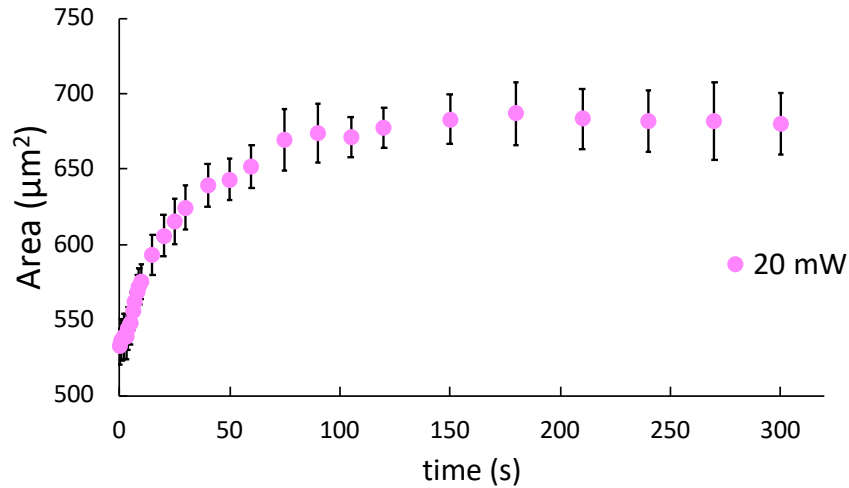


**Figure S3.** Measured pillar area ( $n \geq 11$ ) with a designed diameter of  $20 \mu\text{m}$  and a height of  $30 \mu\text{m}$ , fabricated  $20 \text{ mW}$  laser power upon exposure to  $5 \text{ mM}$  fructose solution (from PBS) over time.

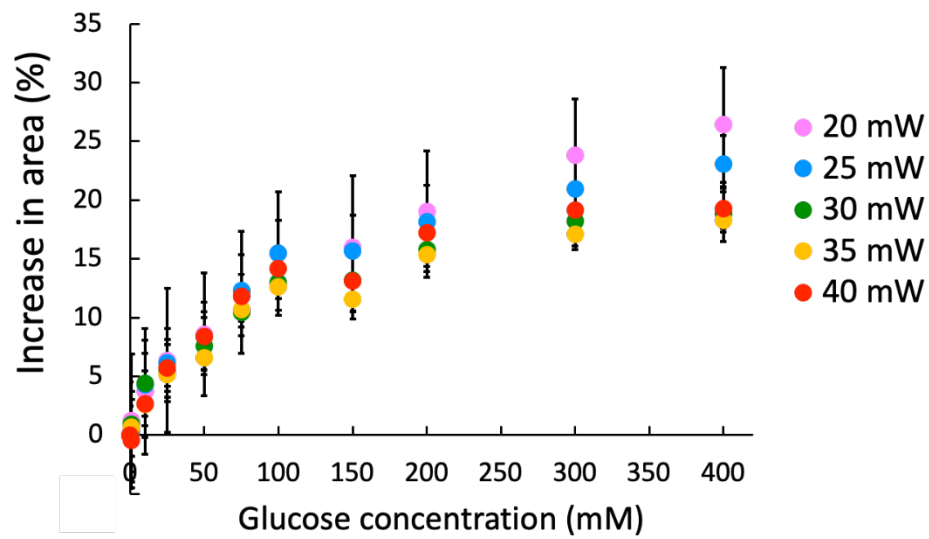


**Figure S4.** Measured pillar area ( $n \geq 11$ ) with a designed diameter of  $20 \mu\text{m}$  and a height of  $30 \mu\text{m}$ , fabricated at different laser powers ( $20 \text{ mW} - 40 \text{ mW}$ ), as the concentration of glucose increases from  $0 \text{ mM}$  (PBS) to  $1 \text{ mM}$ ,  $10 \text{ mM}$ ,  $25 \text{ mM}$ ,  $50 \text{ mM}$ ,  $75 \text{ mM}$ ,  $100 \text{ mM}$ ,  $150 \text{ mM}$ ,  $200 \text{ mM}$ ,  $300 \text{ mM}$  and  $400 \text{ mM}$ .

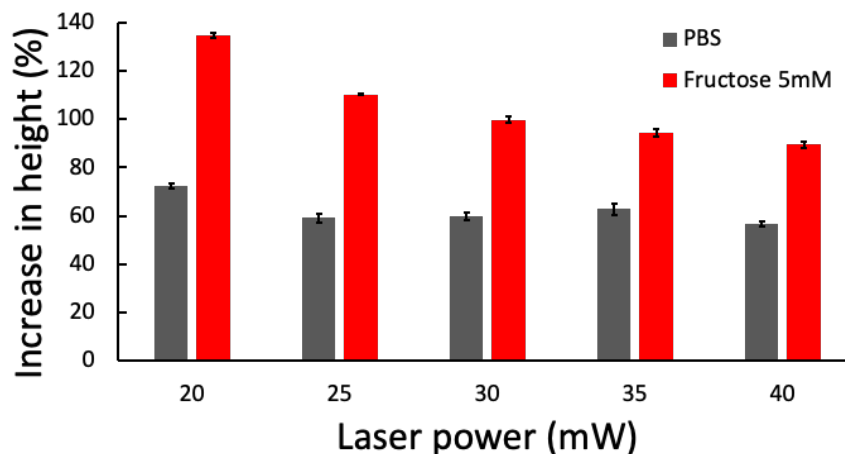


**Figure S5.** Increase in height of cube micro-structures fabricated at different laser powers (20-40 mW) from dry state to PBS (grey) or 5 mM fructose (red), as measured by AFM.

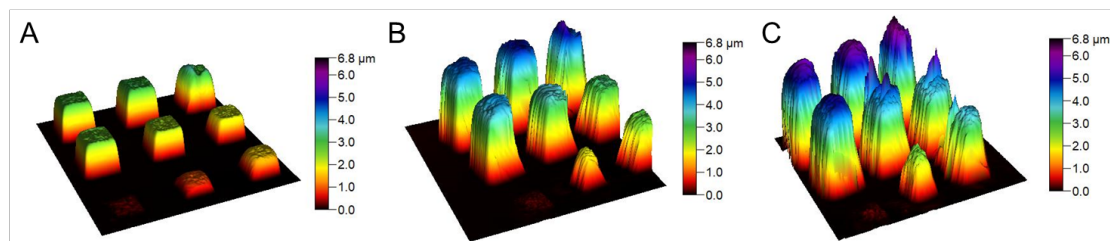


**Figure S6.** 3D height plot of cube array microstructures measured by AFM A) in air; B) in PBS; C) in 5 mM fructose solution in PBS.

**ESI Video S1.** Video showing the swelling of cylindrical pillar structures with the addition of 5 mM fructose from a PBS solution as described in the experimental section. The pillar structures had a design diameter of 20  $\mu\text{m}$  and a design height of 30  $\mu\text{m}$ . The pillars were fabricated using the Photonic Professional GT system (Nanoscribe GmbH) in the oil immersion configuration using a 63X oil objective. The writing parameters were; laser power 25 mW; scan speed 10 mm  $\text{s}^{-1}$ ; slicing 0.3  $\mu\text{m}$ ; hatching 0.3  $\mu\text{m}$ ; no contours. The structures underwent a 22.0%  $\pm$  3.0% increase in area. Video is taken at a z height of 21  $\mu\text{m}$ . Video playback at 10X speed. A selection of images from video S1 are shown below in Figure S7.

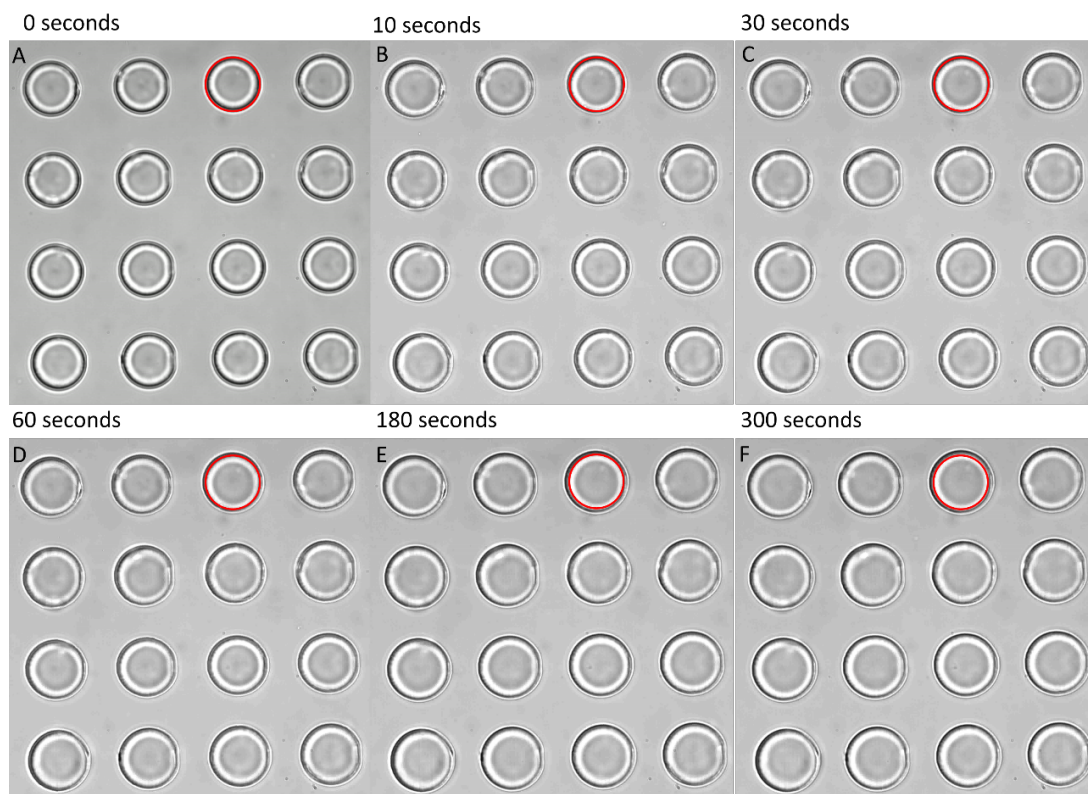


**Figure S7.** Selection of images from Video S1. Marking the pillar structures swelling over time after the addition of a 5 mM fructose solution. The outline of the circumference of the pillar before the addition of 5 mM fructose in PBS is marked in red. The pillar structures had a designed diameter of 20  $\mu\text{m}$  and a designed height of 30  $\mu\text{m}$ . The pillars were fabricated using the Photonic Professional GT system (Nanoscribe GmbH) in the oil immersion configuration using a 63X oil objective. The writing parameters were; laser power 25 mW; scan speed 10 mm s<sup>-1</sup>; slicing 0.3  $\mu\text{m}$ ; hatching 0.3; no contours. A) Image take before the addition of the 5mM fructose solution; B) Image taken 10s after addition of the 5mM fructose solution; C) Image taken 30 seconds after the addition of the 5mM fructose solution; D) Image taken 1 minute after the addition of the 5mM fructose solution; E) Image taken 3 minutes after the addition of the 5mM fructose solution; F) Image taken 5 minutes after the addition of the 5mM fructose solution.

**ESI video S2.** Video showing the swelling of an array of twisted vase structure (same design characterized via confocal microscopy in Figure 4 with the addition of 100 mM fructose. The vase structures were fabricated at a laser power of 25 mW and 20 mm s<sup>-1</sup> with slicing and hatching of 0.3  $\mu\text{m}$ . Video in real time. A selection of images from video S2 are shown below in Figure S8.

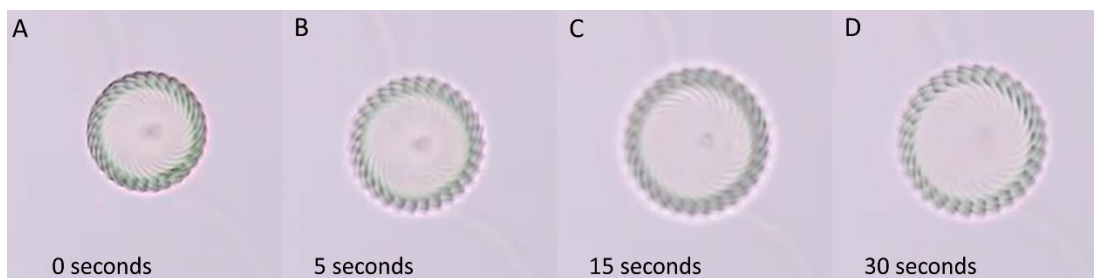


**Figure S8.** Selection of images from Video S2. Showing the swelling of one twisted vase structure over time after the addition of 100 mM fructose solution. The vase structures were fabricated at a laser power of 25 mW and  $20 \text{ mm s}^{-1}$  with slicing and hatching of  $0.3 \mu\text{m}$ . A) Image taken before the addition of fructose solution; B) Image taken 5 seconds after addition of fructose; C) Image taken 15 seconds after addition of fructose. D) Image taken 30 seconds after addition of fructose.

**ESI video S3.** Video of addition of PBS flow to array of twisted vase structures, showing the vase structures actuating under flow and returning to their initial position. All structures were fabricated at 25 mW and  $20 \text{ mm s}^{-1}$ . Video in real time.

**ESI video S4.** Video showing the dry beam structures upon hydration in PBS. The beam is initially bent toward the side fabricated at the lower laser (20 mW) due to the difference in size between the two sides caused by the fabrication parameters. As it swells in PBS the beam bends further towards the side fabricated at lower laser power. The dimensions of the beam are as follows;  $40 \mu\text{m}$  length and each side of the bilayer has a designed width of  $3 \mu\text{m}$ . Writing parameters for the  $10 \times 10 \times 20 \mu\text{m}$  base: laser power 30 mW; scan speed  $5 \text{ mm s}^{-1}$ ; slicing  $0.3 \mu\text{m}$ . Writing parameters for the  $40 \times 6 \times 10 \mu\text{m}$  bilayer beam: Laser power 20 and 25 mW for the two bilayers; scan speed  $4 \text{ mm s}^{-1}$ , slicing in Z direction  $0.3 \mu\text{m}$ . Video speed up 3x times.

**ESI video S5.** Video of bilayer beam structures hydrated in PBS after the addition of 5 mM fructose solution. The beam begins to straighten as the side fabricated at the higher laser power (25 mW) swells less than the side fabricated at the lower laser power (20 mW). Video playback at 3X speed.

**ESI video S6.** Opening of bilayer flower-like structure array hydrated in PBS in response to the addition of 100 mM fructose solution. Inner layer of flower fabricated at a laser power of 20 mW and the outer layer of the structure fabricated at 30 mW; both layers fabricated using a scan speed of  $10 \text{ mm s}^{-1}$ . Video is in real time.

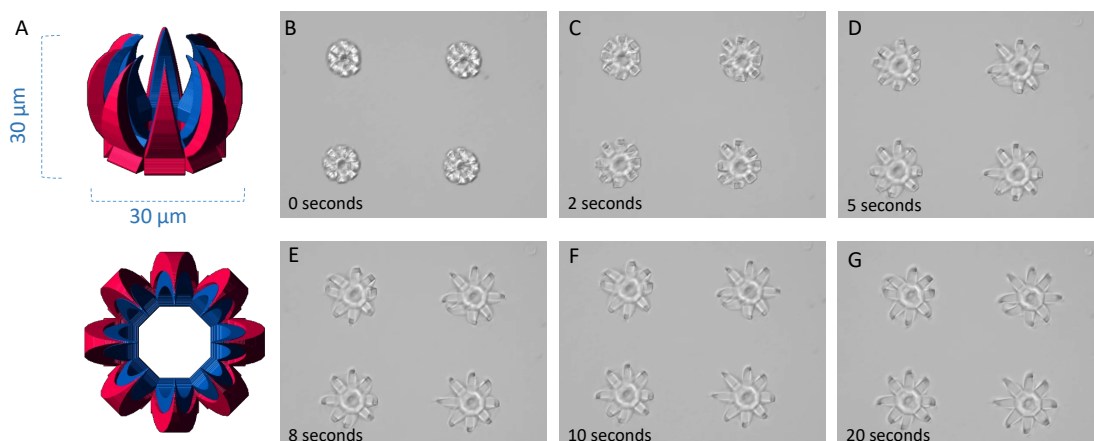


**Figure S9.** Selection of images taken from Video S6 of bilayer flower with a design diameter and height of  $30\ \mu\text{m}$ , opening in response to the addition of  $100\ \text{mM}$  fructose. A) Top and Side view of bilayered structure design, where the inner layer (blue) was fabricated at  $20\ \text{mW}$ , while the outer layer (red) was fabricated at  $30\ \text{mW}$ ; B) Image taken before the addition of fructose; C) Image taken 2 seconds after the addition the fructose solution; D) Image taken 5 seconds after the addition of the fructose solution ; E) Image taken 8 seconds after the addition of fructose solution; F) Image taken 10 seconds after the addition of fructose solution; G) Image taken 20 seconds after the addition of fructose solution.

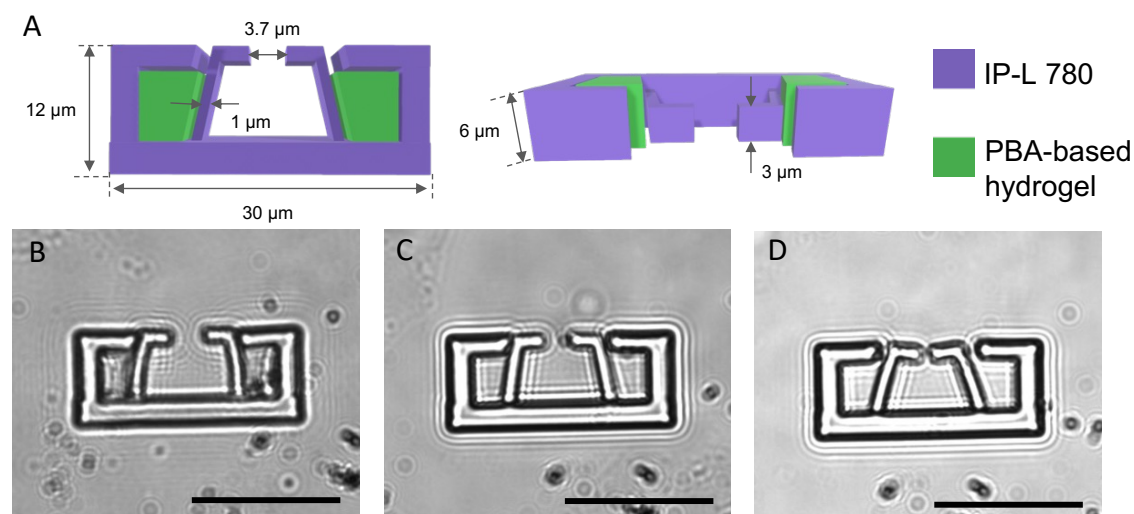


**Figure S10.** Dual-material micro-gripper structure; A) Top (left) and side-view (right) of micro-gripper design showing the design dimensions and the two materials used for fabrication. B-D) Microscope images of the micro-gripper structure in the dry state (B), in PBS (C) and  $100\ \text{mM}$  fructose solution in PBS (D). Images show the micro-gripper arm distance decreasing from  $\sim 3.5\ \mu\text{m}$  in the dry state, to  $\sim 2.8\ \mu\text{m}$  in PBS, with the tips finally meeting in the fructose solution. Scale bar represents  $20\ \mu\text{m}$ .